

# Spin caloritronics as a probe of nonunitary superconductors

Taiki Matsushita\*,<sup>1</sup> Takeshi Mizushima\*,<sup>2</sup> Yusuke Masaki,<sup>3</sup> Satoshi Fujimoto,<sup>2,4</sup> and Ilya Vekhter<sup>5</sup>

<sup>1</sup>Department of Physics, Graduate School of Science, Kyoto University, Kyoto 606-8502, Japan

<sup>2</sup>Department of Materials Engineering Science, Osaka University, Toyonaka, Osaka 560-8531, Japan

<sup>3</sup>Department of Applied Physics, Graduate School of Engineering, Tohoku University, Sendai, Miyagi 980-8579, Japan

<sup>4</sup>Center for Quantum Information and Quantum Biology,  
Osaka University, Toyonaka, Osaka 560-8531, Japan

<sup>5</sup>Department of Physics and Astronomy, Louisiana State University, Baton Rouge, LA 70803-4001, USA

(Dated: April 4, 2024)

Superconducting spintronics focuses on the interplay between superconductivity and magnetism and has sparked significant interest in nonunitary superconductors as a platform for novel magneto-superconducting phenomena. However, a direct test for nonunitary superconductors is currently absent, and their identification is challenging. In this paper, we demonstrate that spin current driven by the thermal gradient sensitively probes the nature of the condensate in nonunitary superconductors. We should note that the spin polarization of the condensate in the momentum space induces the spin-Seebeck effect, and the spin-dependent chirality (spin-chirality) of the condensate induces the spin-Nernst effect in nonunitary superconductors. Notably, the nonvanishing spin-Seebeck effect provides a smoking gun evidence of nonunitary superconductivity in materials because it reflects the spin polarization of the Cooper pairs in the momentum space, irrespective of whether the net pair spin magnetization vanishes. Our results position the spin caloritronics phenomena as a definitive probe of nonunitary superconductors.

## INTRODUCTION

Classification of superconducting states and identification of unusual superconductivity underlie both the efforts to understand mechanisms of electron pairing and applications of superconducting materials. At the most fundamental level, determining whether the superconducting state breaks the time-reversal and/or point group symmetries of the host crystal lattice restricts theories of the pairing in a given family of materials [1–3]. More recently, with the emergence of topological electronic matter as a potential driver for applications, reliable methods to identify topological superconductivity, whether in time-reversal broken or time-reversal invariant states, became an essential question [4–6]. Similarly, proposals to utilize the interplay between superconductivity and magnetism for superconducting spintronics [7–19], brought renewed focus to the studies of the spin properties of the paired electron states.

The superconducting order parameter matrix in spin space,  $\Delta(\mathbf{k}) = [\psi(\mathbf{k}) + \mathbf{d}(\mathbf{k}) \cdot \boldsymbol{\sigma}] (i\sigma_y)$ , where  $\boldsymbol{\sigma} = (\sigma_x, \sigma_y, \sigma_z)$  is a vector of Pauli matrices, has a scalar spin-singlet ( $\psi(\mathbf{k})$ ) and vector spin-triplet ( $\mathbf{d}(\mathbf{k})$ ) components at each momentum  $\mathbf{k}$  at the Fermi surface. The intrinsic spin polarization of the condensate in the momentum space,  $\mathbf{S}(\mathbf{k}) = \text{Tr} [\Delta^\dagger(\mathbf{k}) \boldsymbol{\sigma} \Delta(\mathbf{k})] = -i\mathbf{d}^*(\mathbf{k}) \times \mathbf{d}(\mathbf{k})$ , is inherent in nonunitary superconductors (NUSCs), for which  $\mathbf{d}^*(\mathbf{k}) \times \mathbf{d}(\mathbf{k}) \neq 0$ . However, even if Cooper pairs at each  $\mathbf{k}$  have a well-defined spin polarization, their net pair spin magnetization averaged over the entire Fermi surface may still vanish. Consequently, clear identification of NUSCs remains an outstanding problem.

We show below that the spin current response to the thermal gradient in superconductors provides unique information about the nontrivial structures of the order parameter. Our main conclusion is that the spin-Seebeck effect (SSE), a spin current along the thermal gradient [20–24], provides a smok-

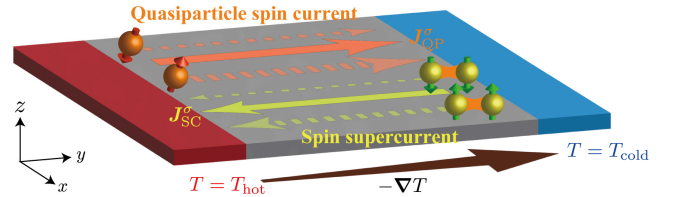


FIG. 1. A sketch of the physical origin of the spin Seebeck effect in nonunitary superconductors. The orange (yellow) arrows show the spin current carried by quasiparticles (Cooper pairs). The broken arrows show the spin-resolved currents. The spin supercurrent is generated to cancel the dissipative electric current carried by quasiparticles, see text for details.

ing gun signature of NUSCs irrespective of whether the net pair spin magnetization vanishes or not. We also emphasize that the spin-Nernst effect (SNE), a spin current perpendicular to the thermal gradient [20, 25, 26], is a probe of the spin-chirality of the condensate [27]. We carry out our calculations in the framework of quasiclassical nonequilibrium Keldysh-Eilenberger theory [28, 29]. The key point of our analysis is that in the bulk of superconductors, the charge thermoelectric current must vanish, but the same condition requires the existence of the spin thermoelectric current in NUSCs, as shown in Fig. 1. Our work demonstrates that spin current is uniquely suited for examining the coupling of the relative orbital motion (the  $\mathbf{k}$ -dependence of the  $\mathbf{d}$ -vector) and the spin (the direction of the  $\mathbf{d}$ -vector) of spin-triplet Cooper pairs.

Our results are relevant to a wide range of superconductors of intense current interest. While early belief was that superconductivity is not compatible with magnetic moments because they break the Cooper pairs [30], currently there are multiple candidates for nonunitary superconductivity. The

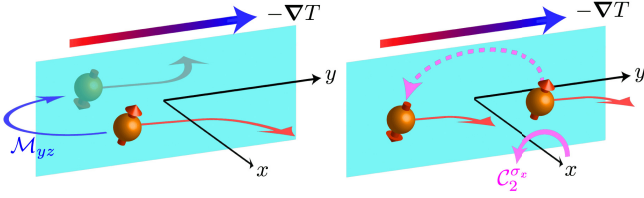


FIG. 2. Schematic images of the operations of the mirror reflection about the  $yz$  plane ( $\mathcal{M}_{yz}$ ) and the two-fold spin rotation about the  $x$  axis ( $C_2^{\sigma_x}$ ).

nonunitary superfluid state is established in  $^3\text{He}$  under applied magnetic fields [31, 32], and nonunitary superconductivity has been proposed in several uranium compounds, such as  $\text{U}_{1-x}\text{Th}_x\text{Be}_{13}$  and  $\text{UTe}_2$ .  $\text{U}_{1-x}\text{Th}_x\text{Be}_{13}$  shows a double superconducting phase transition with decreasing temperature for  $0.19 \leq x \leq 0.40$  [33–35], and its low-temperature phase is strongly suggested to be nonunitary [36–40]. While more controversial, some experiments indicate the possible realization of nonunitary superconductivity in  $\text{UTe}_2$  [41–43]. Ferromagnetic superconductors, such as  $\text{UCoGe}$ ,  $\text{URhGe}$ , and  $\text{UGe}_2$ , where superconductivity emerges from the ferromagnetic metallic phase [44], are also candidates for NUSCs according to the group-theoretical analysis [45]. The nonunitary pairing proposed in Ref [45] successfully explains the angle-resolved NMR experiment in  $\text{UCoGe}$  [46]. As the number of candidate NUSCs increases, we expect that our results will become relevant to a wider and wider range of compounds.

## RESULTS

### Symmetry constraints for the SSE and the SNE

Both the SSE and the SNE must respect discrete symmetries of the system and are generally absent unless such symmetries are broken. We first analyze the SSE and the SNE with the symmetry-based approach. For concreteness, we consider a superconductor in which the thermal gradient ( $-\nabla T$ ) is applied to the  $y$  direction while maintaining spatial uniformity along the  $x$  and  $z$  directions. Let  $\mathcal{T}$ ,  $\mathcal{M}_{yz}$ , and  $C_2^{\sigma_x}$  be the operations of the time-reversal, the mirror reflection in the  $yz$  plane, and the two-fold spin rotation about the  $x$  axis, respectively. As depicted in Fig. 2,  $\mathcal{M}_{yz}$  flips the  $x$  component of the momentum and the  $y$  and  $z$  components of the spin of electrons. i.e.  $(k_x, k_y, k_z) \rightarrow (-k_x, k_y, k_z)$  and  $(\sigma_x, \sigma_y, \sigma_z) \rightarrow (\sigma_x, -\sigma_y, -\sigma_z)$ . Similarly,  $\mathcal{T}$  reverses all components of the spin and the momentum. In contrast,  $C_2^{\sigma_x}$ , which flips only the spin as  $(\sigma_x, \sigma_y, \sigma_z) \rightarrow (\sigma_x, -\sigma_y, -\sigma_z)$ .

With these operations, we derive symmetry constraints for the SSE and the SNE. The spin-Seebeck conductivity (SSC) and the spin-Nernst conductivity (SNC) are defined as,

$$\alpha_{yy}^{\sigma_z} \equiv J_y^{\sigma_z}/(-\partial_y T), \quad \alpha_{xy}^{\sigma_z} \equiv J_x^{\sigma_z}/(-\partial_y T), \quad (1)$$

where  $J_y^{\sigma_z}$  and  $J_x^{\sigma_z}$  are the longitudinal and transverse spin

currents with the spin along the  $z$  direction, respectively. The two-fold spin rotational symmetry ( $C_2^{\sigma_x}$ ) prohibits the spin current responses to the thermal gradient because it ensures equal quasiparticle flow in each of the opposite spin sectors. Note that, in many cases, the broken time-reversal symmetry is required for the SSE, however, the time-reversal symmetry by itself does not prohibit the SSE [47]. Indeed, the SSE with time-reversal symmetry is allowed in some magnetic space groups [48]. The momentum mirror reflection defined as  $\mathcal{M}_{yz}^k = \mathcal{M}_{yz} C_2^{\sigma_x}$  preserves the spin orientation but reverses the transverse momentum,  $k_x \rightarrow -k_x$ . The momentum mirror reflection symmetry ( $\mathcal{M}_{yz}^k$ ) ensures an equal population of quasiparticles with  $k_x > 0$  and  $k_x < 0$  in each spin sector, resulting in  $J_x^{\sigma_z} = 0$ . Therefore, the two-fold spin rotational symmetry must be broken for the SSE and the SNE, and, in addition, the broken momentum mirror reflection symmetry is necessary for the SNE.

### Subsidiary classification of superconducting orders allowing SSE/SNE

We now define subsidiary orders that indicate the breaking of the symmetries prohibiting the SSE and the SNE. It is useful to focus on the angular momentum of Cooper pairs to define the chirality,  $\langle \mathbf{L} \rangle$ , the spin-chirality,  $\langle S_\mu L_\nu \rangle$ , and the pair spin magnetization,  $\langle \mathbf{S} \rangle$ , as [45],

$$\langle \mathbf{L} \rangle = -i \left\langle \hat{d}_\mu^* \left( \mathbf{k}_F \times \frac{\partial}{\partial \mathbf{k}_F} \hat{d}_\mu \right) + \hat{\psi}^* \left( \mathbf{k}_F \times \frac{\partial}{\partial \mathbf{k}_F} \hat{\psi} \right) \right\rangle_{\text{FS}} \quad (2)$$

$$\langle S_\mu L_\nu \rangle = -\frac{i}{2} \sum_{\sigma_\mu = \pm 1} \sigma_\mu \left\langle \hat{\chi}_{\sigma_\mu}^* \left( \mathbf{k}_F \times \frac{\partial}{\partial \mathbf{k}_F} \hat{\chi}_{\sigma_\mu} \right) \right\rangle_{\text{FS}}, \quad (3)$$

$$\langle \mathbf{S} \rangle = -i \langle \hat{d}^* \times \hat{d} \rangle_{\text{FS}}, \quad (4)$$

where the indices  $\mu, \nu = x, y, z$  indicate the vector components,  $\mathbf{k}_F$  is the Fermi momentum and  $\langle \dots \rangle_{\text{FS}}$  is the normalized Fermi surface average (so that  $\langle 1 \rangle_{\text{FS}} = 1$ ). Moreover,  $\hat{d}(\mathbf{k}_F) = \mathbf{d}(\mathbf{k}_F)/\sqrt{\langle |\mathbf{d}(\mathbf{k}_F)|^2 \rangle_{\text{FS}}}$  and  $\hat{\psi}(\mathbf{k}_F) = \psi(\mathbf{k}_F)/\sqrt{\langle |\psi(\mathbf{k}_F)|^2 \rangle_{\text{FS}}}$ , respectively, so that they are independent of the amplitude and the global phase of the superconducting gap. To define the spin chirality, we also introduced the notation  $\hat{\chi}_{\sigma_\mu}(\mathbf{k}_F)$  for the gap function for the Cooper pairs with the spin  $S_\mu = \sigma_\mu$  ( $\sigma_\mu = \pm 1$ ). The explicit form is given by  $\hat{\chi}_{\sigma_\mu}(\mathbf{k}_F) = -\sigma_\mu \hat{d}_\nu(\mathbf{k}_F) + i \hat{d}_\rho(\mathbf{k}_F)$  for  $(\mu, \nu, \rho) = (x, y, z), (y, z, x)$ , and  $(z, x, y)$ .

The chirality is defined as the integral of the orbital angular momentum of the condensate,  $\mathbf{L}$ , over the Fermi surface. It is generated by the complex momentum dependence of the order parameters, such as  $\hat{d}(\mathbf{k}_F)$ ,  $\hat{\psi}(\mathbf{k}_F) \propto (k_x + ik_y)^n$  ( $n \in \mathbb{Z}$ ,  $|n| \geq 1$ ) [63, 64]. Nonvanishing chirality indicates broken time-reversal and mirror reflection symmetries, and induces the polar-Kerr effect, the circular dichroism, the anomalous thermal Hall effect, and the anomalous acoustoelectric effect [55, 64–78].

The spin-chirality and the pair spin magnetization are intrinsic to spinful condensates and thus are common in spin-triplet

Subsidiary order	Breaking symmetries	Candidate materials
Chirality	$\mathcal{T}, \mathcal{M}_{\mu\nu}$	$^3\text{He}$ (A, $A_1^\circ$ and $A_2^\circ$ phases) [31, 32], $\text{Sr}_2\text{RuO}_4$ [49], $\text{URu}_2\text{Si}_2$ [50–52], $\text{SrPtAs}$ [53, 54], $\text{UPt}_3$ (B phase) [49, 55], $\text{U}_{1-x}\text{Th}_x\text{Be}_{13}$ ( $B^\circ$ -phase) [36–40], $\text{UCoGe}^\circ$ [45, 46], $\text{URhGe}^\circ$ [45], $\text{UGe}_2^\circ$ [45]
Spin-chirality	$\mathcal{M}_{\mu\nu}^k, C_2^{\sigma\mu}$	$^3\text{He}$ (B, $A_1^\circ$ , and $A_2^\circ$ phases) phase) [31, 32], $\text{Cu}_x\text{Bi}_2\text{Se}_3$ [56], $\text{U}_{1-x}\text{Th}_x\text{Be}_{13}$ (A, $B^\circ$ and C phase) [36–40, 57, 58], $\text{UCoGe}^\circ$ [45, 46], $\text{URhGe}^\circ$ [45], $\text{UGe}_2^\circ$ [45], $\text{UTe}_2$ [59–62], $\text{URhGe}^\circ$ [45], $\text{UGe}_2^\circ$ [45]
Pair spin magnetization	$\mathcal{T}, C_2^{\sigma\mu}$	$^3\text{He}$ ( $A_1^\circ$ and $A_2^\circ$ phase) [31, 32], $\text{U}_{1-x}\text{Th}_x\text{Be}_{13}$ ( $B^\circ$ -phase) [36–40], $\text{UCoGe}^\circ$ [45, 46], $\text{URhGe}^\circ$ [45], $\text{UGe}_2^\circ$ [45]

TABLE I. The subsidiary orders, the corresponding broken symmetries, and the candidate materials.  $\circ$  represents the nonunitary superconducting phase.

superconductors. The elements of the spin-chirality tensor are the components of the spin-dependent chirality. They generically appear when the  $d$ -vector has multi-component and changes its direction in the spin space depending on the momentum on the Fermi surface. To illustrate this, we consider helical superconducting order with  $\hat{d} \propto (k_x, k_y, 0)$ . This order parameter describes Cooper pairs with  $L_z = \pm 1$  and  $S_z = \mp 1$ , yielding nonvanishing spin-chirality element,  $\langle S_z L_z \rangle$  [27]. Because the chirality breaks the mirror-reflection symmetry, the spin-chirality explicitly breaks the two-fold spin-rotational and momentum mirror-reflection symmetries, allowing the SNE.

Finally, as discussed above, the pair spin magnetization only exists in NUSCs [45], albeit not all such superconductors have the finite pair spin magnetization. Nonvanishing pair spin magnetization explicitly breaks the time-reversal and two-fold spin-rotational symmetries, immediately allowing the SSE. However, we show below that this is a sufficient, but not a necessary condition for nonzero SSC.

Table. I summarizes the candidate materials with the finite subsidiary superconducting orders.

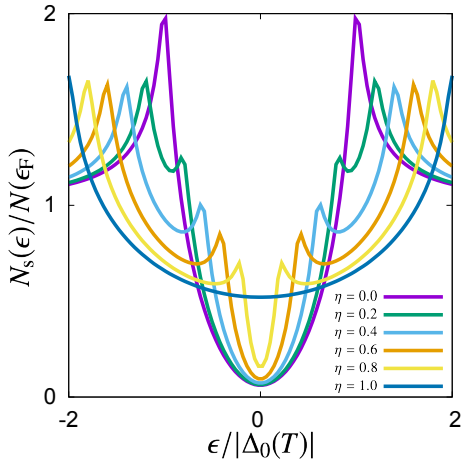


FIG. 3. The density of states (DOS) of the superconducting state described by Eq. (5) with several values of  $\eta$ . Here,  $N(\epsilon_F)$  is the DOS at the Fermi level in the normal state. For the calculation, we set the temperature  $T = 0.1T_c$ , the normal scattering rate  $\Gamma_{\text{imp}} = 0.04\pi T_c$ , and the normal state scattering phase shift  $\delta = \pi/6$ .

### Nonunitary superconductor with finite pair spin magnetization

We first demonstrate that the finite pair spin magnetization,  $\langle S \rangle \neq 0$ , induces the SSE in NUSCs. We assume a spherical Fermi surface of radius  $k_F$  and the  $d$ -vector of the form,

$$\mathbf{d}(\mathbf{k}) = \Delta_0(T)(\hat{k}_x + i\hat{k}_y, \eta(\hat{k}_y - i\hat{k}_x), 0), \quad (5)$$

with  $\hat{k} = \mathbf{k}/k_F$ . Here,  $\Delta_0(T)$  is the gap amplitude and we model its temperature dependence by  $\sqrt{\langle |d(\mathbf{k})|^2 \rangle_{\text{FS}}} = \sqrt{2(1+\eta^2)/3}|\Delta_0(T)| = 1.765T_c \tanh(1.74\sqrt{T_c/T} - 1)$ , where  $T_c$  is the superconducting transition temperature [30, 79].

We obtain the subsidiary orders generated by the superconducting order parameter in Eq. (5) as,

$$\langle L_z \rangle = 1, \quad \langle S_z L_z \rangle = \langle S_z \rangle = -\frac{2\eta}{1+\eta^2}. \quad (6)$$

Equation (5) describes the NUSCs with the pair spin magnetization when  $\eta \neq 0$ . In this case, the superconducting gap amplitudes are different for different spin orientations,  $|\chi_{\sigma_z}(\mathbf{k}_F)| \propto |-\sigma_z + \eta|$ . This splitting is shown in Fig. 3, where the density of states (DOS) has two distinct peaks for finite  $\eta$ . These spin-dependent gap amplitudes make possible nonvanishing spin-chirality and pair spin magnetization.

The details of our linear response calculation are given in the Methods section. Using the quasiclassical (Eilenberger) approach, we compute the dissipative electric current,  $\mathbf{J}_{\text{QP}}$ , carried by quasiparticles driven by the thermal gradient. In the Eilenberger theory, such thermoelectric current appears via the effective particle-hole anisotropy due to the impurity potential [27], which arises from the impurity vertex corrections upon inclusion of the multiple scattering processes. It is important to note that the thermoelectric current is subject to the reaction from the supercurrent,  $\mathbf{J}_{\text{SC}}$ . Indeed, the magnetic flux is excluded from the bulk according to the London equation,  $\nabla^2 \mathbf{B} = \mathbf{B}/\lambda^2$ , where  $\lambda$  is the magnetic penetration depth. This exclusion of the magnetic flux significantly suppresses the thermoelectric response [80] because the magnetic flux is associated with the electric current via the Maxwell-Ampère relation,  $\mathbf{J}_{\text{QP}} + \mathbf{J}_{\text{SC}} = \nabla \times \mathbf{B}$ . When the Meissner effect is complete,  $\mathbf{B} = 0$ , the thermoelectric current vanishes,  $\mathbf{J}_{\text{QP}} + \mathbf{J}_{\text{SC}} = 0$ . In other words, the thermal gradient induces the spatial variation of the phase of the superconducting

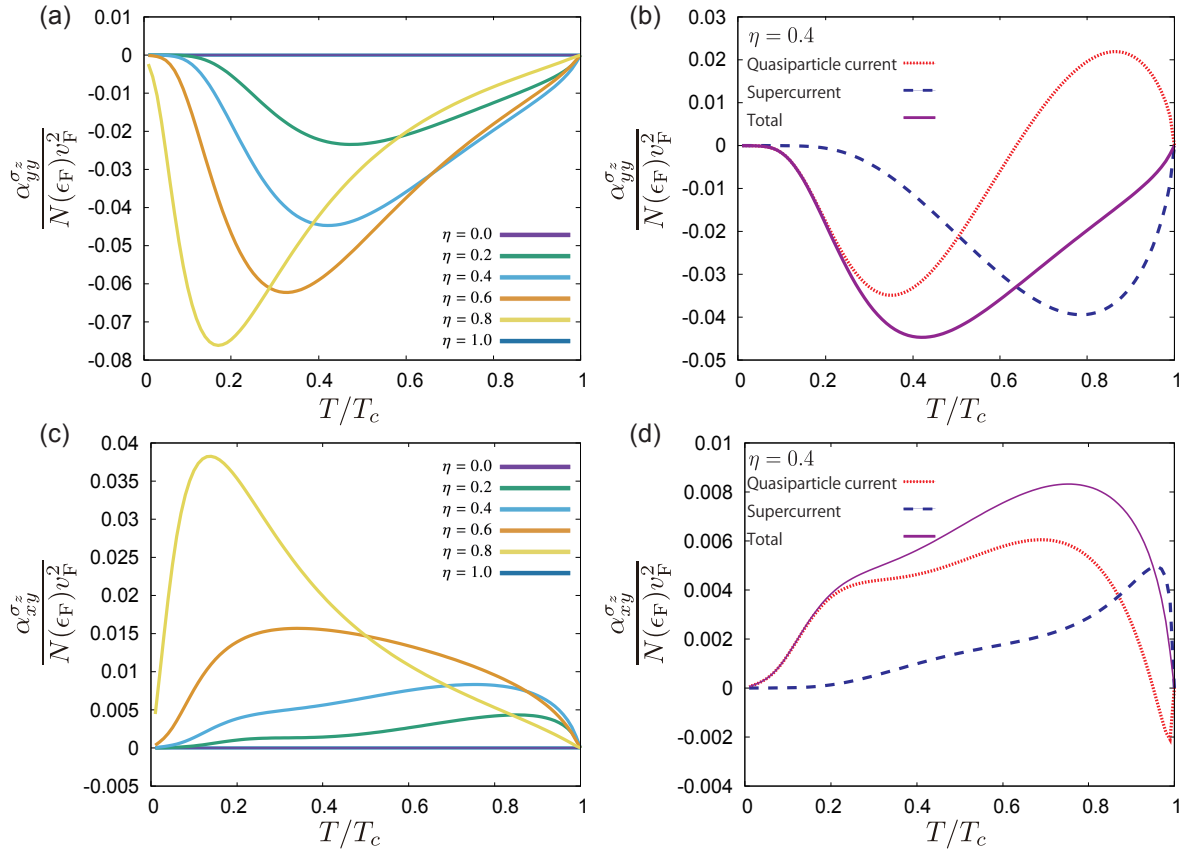


FIG. 4. The temperature dependence of (a-b) the spin-Seebeck conductivity and (c-d) the spin-Nernst conductivity of the superconducting state described by Eq. (5). In the panels (a) and (c), the calculated results with the several values of  $\eta$  are shown. In the panels (b) and (d), The contributions from the quasiparticle current (the red dotted curves), the supercurrent as a reaction of the dissipative electric current (the dashed blue curves), and the total of these (the solid purple curves) are described when  $\eta = 0.4$ . In all panels, we set  $\Gamma_{\text{imp}} = 0.04\pi T_c$  and  $\delta = \pi/6$  for the calculations.

gap that drives the additional supercurrent which compensates the dissipative thermoelectric current carried by quasiparticles [81]. To account for this, we introduce the phase variation into the equilibrium superconducting order according to  $\Delta(\mathbf{k}_F) \rightarrow e^{i\mathbf{Q}\cdot\mathbf{x}}\Delta(\mathbf{k}_F)$  and choose  $\mathbf{Q}$  such that  $\mathbf{J}_{\text{QP}} + \mathbf{J}_{\text{SC}} = 0$ . Remarkably, with this choice, the nontrivial spin response survives.

Figure 4 (a) demonstrates that the SSE is induced by the pair spin magnetization generated by the finite  $\eta$ . The SSE is absent in the unitary case ( $\eta = 0$ ), where the two-fold spin rotational symmetry about the  $x$  axis is recovered. Note that the SSE is also absent in the fully polarized case,  $\eta = 1$ , where only a single gap in one spin channel remains,  $\hat{\chi}_{\sigma_z=+1} = 0$ . In this situation, the electric current is proportional to the spin current, and hence the cancellation of the thermoelectric response by the supercurrents leads to vanishing of the spin current as well. Thus, the SSE in NUSCs exists only in cases of the partial spin polarization of the condensate. As an example, in Fig. 4 (b), we show that the reaction of the supercurrent does not fully cancel the spin current carried by quasiparticles when  $\eta = 0.4$ .

Figure 4 (c) demonstrates that the spin-chirality generated

by the finite  $\eta$  induces the SNE in NUSCs. Quite generally, the anomalous transverse transport arises from the asymmetry of the skew scattering of quasiparticles at impurity sites. Such asymmetry emerges from the impurity vertex corrections when the condensate has the chirality [71–74], and hence the spin-chirality leads to transverse spin transport, i.e. the SNE [27]. As shown in Fig. 4 (c), the SNE is absent when  $\eta = 0$ , where the spin-chirality vanishes. Note also that the anomalous Nernst effect, a electric current perpendicular to the thermal gradient, is once again subject to the reaction of the supercurrent and vanishes in the bulk. As shown in Fig. 4 (d), this reaction of the supercurrent to the anomalous Nernst effect modifies the SNE in NUSCs. Similarly to the SSE, the SNE is also fully canceled by the supercurrent when the spin polarization is complete.

#### Nonunitary superconductor without the pair spin magnetization

We finally demonstrate that the SSE is generic in NUSCs even in the absence of the net pair spin magnetization. As

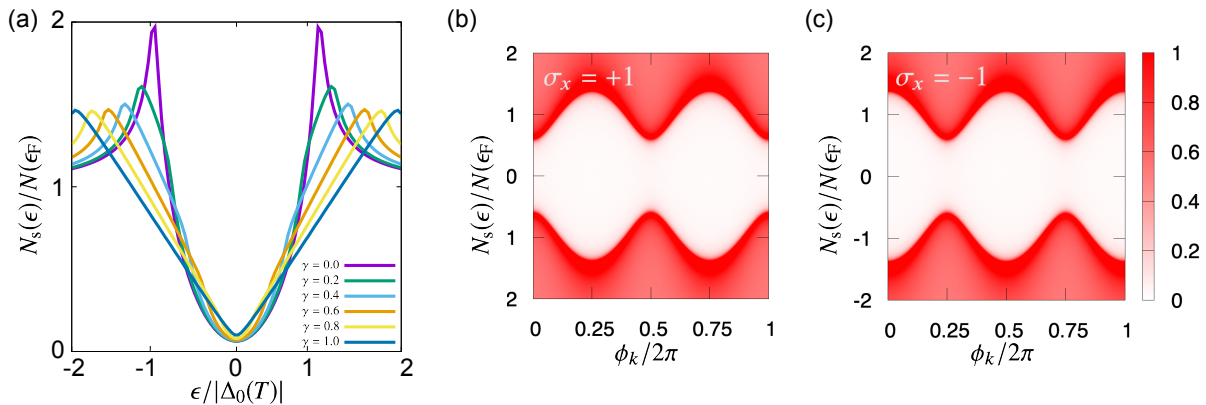


FIG. 5. (a) The density of states (DOS) of the superconducting state described by Eq. (7) with several values of  $\gamma$ . (b-c) The spectral function in the  $k_x = 0$  plane of the superconducting state described by Eq. (7), where  $\phi_k = \tan^{-1}(k_y/k_z)$  and  $\gamma = 0.4$ . In all panels, we set  $T = 0.1T_c$ ,  $\Gamma_{\text{imp}} = 0.04\pi T_c$  and  $\delta = \pi/6$  for the calculations.

an example, we consider the following  $d$ -vector on the Fermi sphere,

$$\mathbf{d}(\mathbf{k}) = \Delta_0(T)(0, \hat{k}_z + i\gamma\hat{k}_y, \hat{k}_y + i\gamma\hat{k}_z), \quad (7)$$

and again assume  $\sqrt{\langle |d(\mathbf{k})|^2 \rangle_{\text{FS}}} = \sqrt{2(1+\gamma^2)/3}|\Delta_0(T)| = 1.765T_c \tanh(1.74\sqrt{T_c/T-1})$  [30].

When  $\gamma \neq 0$ , Eq. (7) describes the nonunitary state, but the spin polarization of the Cooper pairs,  $S_x(\mathbf{k}) \propto (\hat{k}_z^2 - \hat{k}_y^2)$ , vanishes after the integration over the Fermi surface. As is shown in Fig. 5, the coherence peaks in the DOS do not split, but the spectrum depends on the spin. For  $\gamma > 0$ , the  $\sigma_x = +1$  ( $\sigma_x = -1$ ) spin pairing sector has the nodal excitation along the  $z$  ( $y$ ) direction.

Figure 6 (a) demonstrates that this spin-dependent spectrum induces the SSE. The thermal gradient along the  $z$  direction excites quasiparticles in the  $\sigma_x = +1$  sector more than those in the  $\sigma_x = -1$  sector, and hence gives rise to the SSE after taking into account for the cancellation of the electric current. This illustrates the essential point of our analysis: in NUSCs, the quasiparticle spectrum along a given direction is different for the opposite spin projections on the spin quantization axis. In a generic case, the spin and electric currents are different for a given direction of the thermal gradient, and hence the SSE emerges even when the thermoelectric current vanishes due to the reaction of the supercurrent. Note that the supercurrent still carries the spin even in the absence of the net spin magnetization. This behavior is shown in Fig. 6 (b) and the reaction of the supercurrent modifies the SSE even when the pair spin magnetization is absent. For completeness, we also show the spin-Nernst effect in Fig. 6 (c-d).

## DISCUSSION

The model order parameters considered above are motivated by recent proposals relevant to the intensely studied unconventional superconductors. The  $d$ -vector in Eq. (5) is

established in the  $A_1$  and  $A_2$  phases of the superfluid  $^3\text{He}$  under applied magnetic fields [31, 32]. In the superfluid  $^3\text{He}$ , the interplay between unconventional pairing and quasiparticle impurity scattering can be engineered by high-porosity silica aerogel [82]. The aerogel, which is modeled by randomly distributed nonmagnetic impurities with  $\delta \approx \pi/2$  and  $\Gamma_{\text{imp}} \approx 0.1 - 0.2\pi T_c$  [83], realizes the  $A_1$  and  $A_2$  phases under magnetic fields [84]. Although the calculated results with Eq. (5) can be applied to these phases, the effects of the spin supercurrent and the collective motion of the  $d$ -vector have yet to be explored.

The  $d$ -vector in Eq. (5) has been suggested for UCoGe, where superconductivity coexists with ferromagnetically ordered moments along the  $z$  direction [44]. Since superconductivity emerges from this ferromagnetic state, the spin of the condensate must be aligned along the same direction so that  $\langle S_z \rangle$  is realized [45]. The NMR measurement supports the realization of the  $A_1$  state described by  $\mathbf{d}(\mathbf{k}) = (a_1k_x + ia_2k_y, a_3k_y + ia_4k_x, 0)$ , where  $a_i$  ( $i = 1, 2, 3, 4$ ) are real coefficients [46]. Equation (5) is obtained if we set  $a_1 = a_2$ ,  $a_3/a_1 = -a_4/a_1 = \eta$  and thus our results with Eq. (5) can be directly applied to UCoGe.

The main caveat is that strongly ferromagnetic superconductors may support a spontaneous vortex state [85, 86]. In such cases, the Meissner screening is not only incomplete, but vortices generate unpaired quasiparticles, and vortex motion contributes to the transverse transport. Nonetheless, in the majority of ferromagnetic superconductors, the evidence for the spontaneous vortex state is scant, and thus we believe that our results are applicable.

If the exchange splitting is large enough to make the difference in e.g. Fermi velocities between the two spin orientations substantial, we may expect corrections to the quasiclassical results. However, in most materials under discussion, the splitting is small and appears as a higher order correction in the powers of  $(k_F\xi_0)^{-1} \ll 1$ , where  $\xi_0$  is the superconducting coherence length.

Another notable candidate for spin-triplet superconductivity is  $\text{UTe}_2$ , which exhibits a very large upper critical magnetic

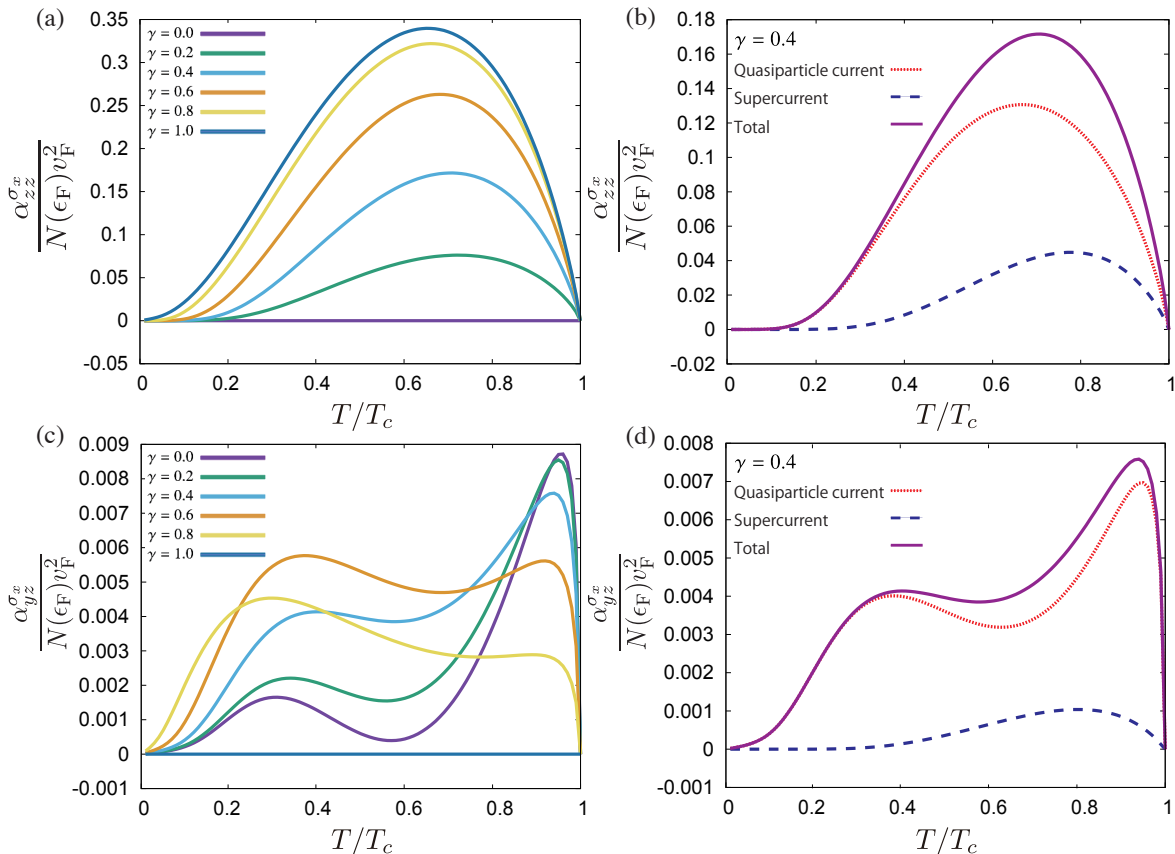


FIG. 6. The temperature dependence of (a-b) the spin-Seebeck conductivity and (c-d) the spin-Nernst conductivity of the superconducting state described by Eq. (5). In the panels (a) and (c), the calculated results with the several values of  $\gamma$  are shown. In the panels (b) and (d), the quasiparticle current (the red dotted curves), the supercurrent as a reaction of the dissipative electric current (the dashed blue curves), and the total of these (the solid purple curves) are shown for  $\gamma = 0.4$ . In all panels, we set  $\Gamma_{\text{imp}} = 0.04\pi T_c$  and  $\delta = \pi/6$  for the calculations.

field (over 30 T) and strong magnetic Ising anisotropy [59, 60]. These features strongly support spin-triplet superconductivity in  $\text{UTe}_2$ . Early on there were indications that non-unitary superconductivity may be realized in this compound. Observation of polar Kerr signal below  $T_c$  suggesting realization of a superconducting order with the broken time-reversal symmetry [42]. Furthermore, the magnetic field penetration depth measurement supported the realization of the  $\text{B}_{3u} + iA_u$  state, which is nonunitary [43]. However, more recent experiments with high-quality samples failed to observe the polar Kerr signal in  $\text{UTe}_2$  in the absence of magnetic fields, and therefore currently the nonunitary superconductivity in  $\text{UTe}_2$  is still a subject of debate [87]. Our results above may help to settle this question.

Note that the  $\text{B}_{3u} + iA_u$  state is described by  $\mathbf{d}(\mathbf{k}) = (a_1 k_x, b_1 k_z + ia_2 k_y, b_2 k_y + ia_3 k_z)$ , where  $a_i$  ( $i = 1, 2, 3$ ) are the coefficients for the basis function of the  $A_u$  representation and  $b_i$  ( $i = 1, 2$ ) are coefficients for the basis function of the  $\text{B}_{3u}$  representation, respectively [43]. Recent theoretical analysis argued that strong magnetic Ising anisotropy suppresses the  $x$  component of the  $d$ -vector in

$\text{UTe}_2$  [88]. When we combine these results and then set  $a_1 = 0$ ,  $b_2 = b_3$ ,  $a_2/b_2 = a_3/b_3 = \gamma$ , the  $d$ -vector reduces to Eq. (7). Consequently, our model is directly applicable to the candidate orders in  $\text{UTe}_2$ .

Note that  $\text{UTe}_2$  is paramagnetic above  $T_c$  (albeit it may be close to a ferromagnetic phase), which excludes the spontaneous vortex state. The SSE is thus useful as a test for nonunitary superconductivity in  $\text{UTe}_2$ .

In our calculations, the existence of the SSE and the SNE relies on the asymmetries of impurity scattering due to the structure of the order parameter. In principle, the particle-hole anisotropy in the normal state leads to similar asymmetries [75, 89–91] and may dominate for sufficiently clean samples. However, in the weak coupling regime, this effect is again of order  $(k_F \xi_0)^{-1} \ll 1$ , and therefore in realistic materials, we expect that the impurity mechanism is dominant.

## CONCLUSION

In summary, we showed that the SSE is a generic feature of NUSCs irrespective of whether the superconducting con-

densate has the net pair spin magnetization. We placed our results in the context of symmetries broken by the subsidiary classification of the order parameters with respect to the chirality, the spin-chirality, and the pair spin magnetization. Together with the transverse counterpart of the SSE, the SNE, which is sensitive to the spin-chirality and tests for the helical superconducting order in time-reversal-invariant topological superconductors [27], our work establishes spin caloritronics phenomena as sensitive probes of the symmetries of the order parameters in spin-triplet superconductors. We argued for the possible relevance of our detailed calculations to measurements in UTe<sub>2</sub> and U-based ferromagnetic superconductors, but our broader picture remains applicable to a wide range of currently known and future NUSCs.

## MATERIALS AND METHOD

### Quasiclassical Eilenberger theory of superconductivity

The quasiclassical method in the theory of superconductivity relies on the small parameter,  $(k_F \xi_0)^{-1} \sim T_c / \epsilon_F$ , in superconductors, where  $\epsilon_F$  is the Fermi energy [28, 29], to develop an approximation scheme for the Green function. To formulate the spin current responses to the thermal gradient, we consider the Green function,  $\check{G}$ , in the spin, particle-hole (Nambu), and time-ordered Keldysh space. When  $(k_F \xi_0)^{-1} \ll 1$ , all the elements of the Green function are sharply peaked at the Fermi energy and weakly depend on the energy far away from it. The high-energy (away from the Fermi surface) part of  $\check{G}$  renormalizes interactions between electrons. The low-energy part determines the equilibrium properties and response to external perturbations. The essence of this method is to define the quasiclassical Keldysh Green function,  $\check{g}(\epsilon, \mathbf{k}_F)$ , as the integral of  $\check{G}$  over energy, so that the major contribution comes from the vicinity of the Fermi surface.

To implement this approach, we linearize the dispersion of normal electrons near the Fermi energy,  $\xi_{\mathbf{k}} = v_F \cdot (\mathbf{k} - \mathbf{k}_F)$ , with the Fermi velocity  $v_F \equiv (\partial \xi_{\mathbf{k}} / \partial \mathbf{k})_{\mathbf{k}=\mathbf{k}_F}$ , and then the quasiclassical Green function,  $\check{g}$ , is defined in the Keldysh space as [92],

$$\check{g}(\epsilon, \mathbf{k}_F) = \begin{pmatrix} \underline{g}^R(\epsilon, \mathbf{k}_F) & \underline{g}^K(\epsilon, \mathbf{k}_F) \\ 0 & \underline{g}^A(\epsilon, \mathbf{k}_F) \end{pmatrix} \equiv \int_{-\epsilon_c}^{\epsilon_c} d\xi_{\mathbf{k}} \check{\tau}_z \check{G}(\epsilon, \mathbf{k}), \quad (8)$$

where  $\check{\tau}_\mu$  ( $\mu = x, y, z$ ) are the Pauli matrices in the particle-hole space and  $\epsilon_c$  is the cutoff energy satisfying  $T_c \ll \epsilon_c \ll \epsilon_F$ . The superscripts, X = R, A, K, represent the retarded, advanced and Keldysh components. Each of these components, in turn, is a matrix in the spin and particle-hole space,

$$\underline{g}^X = \begin{pmatrix} g^X + \mathbf{g}^X \cdot \boldsymbol{\sigma} & [\boldsymbol{\sigma} \cdot \mathbf{f}^X](i\sigma_y) \\ (i\sigma_y)[\boldsymbol{\sigma} \cdot \bar{\mathbf{f}}^X] & \bar{g}^X - \sigma_y \bar{\mathbf{g}}^X \cdot \boldsymbol{\sigma} \sigma_y \end{pmatrix}, \quad (9)$$

where  $\boldsymbol{\sigma} = (\sigma_x, \sigma_y, \sigma_z)$  is the vector of the Pauli matrices in the spin space.  $g^X$  and  $\bar{g}^X$  ( $\mathbf{g}^X$  and  $\bar{\mathbf{g}}^X$ ) are the spin scalar

(vector) components of the electron and hole propagators,  $f^X$  and  $\bar{f}^X$  are the spin-triplet electron and hole pair amplitudes, respectively. Throughout the manuscript, we denote a matrix in the Keldysh space as  $\check{A}$  and a matrix in the spin and particle-hole space as  $\underline{A}$ .

The quasiclassical Green function obeys the standard Eilenberger equation,

$$[\epsilon \check{\tau}_z - \check{\Delta}(\mathbf{k}_F) - \check{\sigma}_{\text{imp}}, \check{g}] + i v_F \cdot \nabla \check{g} = 0, \quad (10)$$

supplemented by the normalization condition,  $\check{g}^2 = -\pi^2$  [28, 29].  $\check{\Delta}(\mathbf{k}_F)$  in Eq. (10) is the mean-field pairing self-energy. In spin-triplet superconductors,  $\check{\Delta}(\mathbf{k}_F)$  is associated with the  $d$ -vector as,

$$\check{\Delta}(\mathbf{k}_F) = \begin{pmatrix} \underline{\Delta}(\mathbf{k}_F) & 0 \\ 0 & \underline{\Delta}(\mathbf{k}_F) \end{pmatrix}, \quad (11a)$$

$$\begin{aligned} \underline{\Delta}(\mathbf{k}_F) &= \begin{pmatrix} 0 & \Delta(\mathbf{k}_F) \\ -\Delta^\dagger(\mathbf{k}_F) & 0 \end{pmatrix} \\ &= \begin{pmatrix} 0 & \mathbf{d}(\mathbf{k}_F) \cdot \boldsymbol{\sigma}(i\sigma_y) \\ \mathbf{d}^*(\mathbf{k}_F) \cdot (i\sigma_y)\boldsymbol{\sigma} & 0 \end{pmatrix}, \end{aligned} \quad (11b)$$

where  $\Delta(\mathbf{k}_F) = \mathbf{d}(\mathbf{k}_F) \cdot \boldsymbol{\sigma}(i\sigma_y)$  is the order parameter matrix in the spin space. When the  $d$ -vector satisfies  $\mathbf{d}^*(\mathbf{k}) \times \mathbf{d}(\mathbf{k}) = \mathbf{0}$ , the pairing states are referred to as unitary because  $\Delta^\dagger(\mathbf{k}_F)\Delta(\mathbf{k}_F) = |\mathbf{d}(\mathbf{k}_F)|^2$ . Otherwise, the pairing states are referred to as nonunitary with  $\Delta^\dagger(\mathbf{k}_F)\Delta(\mathbf{k}_F) = |\mathbf{d}(\mathbf{k}_F)|^2 + i(\mathbf{d}^*(\mathbf{k}_F) \times \mathbf{d}(\mathbf{k}_F)) \cdot \boldsymbol{\sigma}$  [1]. As discussed in the main text and shown in Eq. (4),  $\mathbf{S}(\mathbf{k}) = -i\mathbf{d}^*(\mathbf{k}) \times \mathbf{d}(\mathbf{k})$  describes the spin polarization of the condensate in the momentum space and lifts the spin-degeneracy in the quasiparticle spectrum.

The impurity effects are incorporated in the impurity self-energy,  $\check{\sigma}_{\text{imp}}$ . In the quasiclassical theory, the impurity effects are essential for obtaining nonvanishing SSE and SNE. These transport coefficients require particle-hole asymmetry [75, 89]. While this asymmetry may arise simply from the density of states, [90, 91], such effects are small for  $(k_F \xi_0)^{-1} \ll 1$ , and are neglected in the Eilenberger theory. However, in superconductors, the particle-hole anisotropy also appears via the impurity vertex corrections with the inclusion of the multiple scattering processes [27].

We adopt the self-consistent  $T$ -matrix approximation (SCTMA) to compute the impurity self-energy, which contains all of the non-crossing diagrams associated with the multiple scattering processes (Fig. 7). We assume randomly distributed nonmagnetic impurities with the short-range impurity potential with the potential strength,  $V_{\text{imp}}$ , and the impurity density,  $n_{\text{imp}}$ . In the SCTMA, the impurity self-energy is [93],

$$\check{\sigma}_{\text{imp}} = \begin{pmatrix} \underline{\sigma}_{\text{imp}}^R & \underline{\sigma}_{\text{imp}}^K \\ 0 & \underline{\sigma}_{\text{imp}}^A \end{pmatrix} = -\Gamma_{\text{imp}} \left( \cot \delta + \left\langle \frac{\check{g}}{\pi} \right\rangle_{\text{FS}} \right)^{-1}, \quad (12)$$

where  $\Gamma_{\text{imp}} = n_{\text{imp}} / (\pi N(\epsilon_F))$  is the normal-state scattering rate and  $\cot \delta = -1 / (\pi N(\epsilon_F) V_{\text{imp}})$  is the scattering phase shift. These quantities are defined in the normal state and parameterize impurity scattering in our calculations.

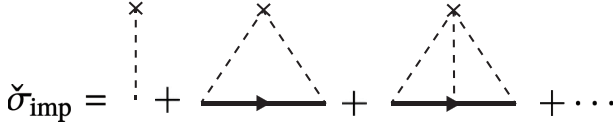


FIG. 7. The Feynman diagrams for the impurity self-energy with the self-consistent  $T$ -matrix approximation.

We consider the dilute impurity limit,  $\Gamma_{\text{imp}} \ll T_c$ . Spin-triplet superconductivity is fragile with respect to the disorder, but for  $\Gamma_{\text{imp}} \ll T_c$ , the reduction of  $T_c$  is small even when the impurity potential is strong,  $\cot \delta \rightarrow 0$  [94].

### Response to a thermal gradient

We now formulate the response theory to the thermal gradient within the framework of the Eilenberger theory [95, 96]. The formalism is simplified in the cases when the  $d$ -vector has only two components as in Eq. (5) and Eq. (7). In these cases, we can choose a spin quantization axis along which the order parameter matrix is diagonalized in the spin space. For example, for  $\mathbf{d}(\mathbf{k}) = (d_x, d_y, 0)$ , the appropriate quantization axis is the  $z$  axis. Let us denote such an axis as  $\mu$  and then the quasiclassical Green function is also block-diagonal in the spin space,  $\check{g} = \check{g}^{\sigma_\mu=+1} \oplus \check{g}^{\sigma_\mu=-1}$ , because both nonmagnetic impurities and the thermal gradient do not break the spin conservation.

In each spin sector, we separate  $\check{g}^{\sigma_\mu}$  into the equilibrium part,  $\check{g}_{\text{eq}}^{\sigma_\mu}$ , and its deviation from the equilibrium,  $\delta\check{g}^{\sigma_\mu} = \check{g}^{\sigma_\mu} - \check{g}_{\text{eq}}^{\sigma_\mu}$ , which linearly depends on the thermal gradient. The equilibrium quasiclassical Green function obeys the homogeneous Eilenberger equation,

$$\left[ \epsilon \check{\tau}_z - \check{\Delta}_{\text{eq}}^{\sigma_\mu}(\mathbf{k}_F) - \check{\sigma}_{\text{imp,eq}}^{\sigma_\mu}, \check{g}_{\text{eq}}^{\sigma_\mu} \right] = 0, \quad (13)$$

where the brackets denote a commutator. This equation is supplemented by the normalization condition,  $[\check{g}_{\text{eq}}^{\sigma_\mu}]^2 = -\pi^2$ . Here,  $\check{\Delta}_{\text{eq}}^{\sigma_\mu}$  is the mean-field pairing self-energy in the spin sector  $\sigma_\mu$  and is associated with  $\check{\Delta}_{\text{eq}}$  as  $\check{\Delta}_{\text{eq}} = \check{\Delta}_{\text{eq}}^{\sigma_\mu=+1} \oplus \check{\Delta}_{\text{eq}}^{\sigma_\mu=-1}$ .  $\check{\Delta}_{\text{eq}}^{\sigma_\mu}$  has the form,

$$\check{\Delta}_{\text{eq}}^{\sigma_\mu}(\mathbf{k}_F) = \begin{pmatrix} \Delta_{\text{eq}}^{\sigma_\mu}(\mathbf{k}_F) & 0 \\ 0 & \underline{\Delta}_{\text{eq}}^{\sigma_\mu}(\mathbf{k}_F) \end{pmatrix}, \quad (14a)$$

$$\underline{\Delta}_{\text{eq}}^{\sigma_\mu}(\mathbf{k}_F) = \begin{pmatrix} 0 & \Delta_{\text{eq}}^{\sigma_\mu}(\mathbf{k}_F) \\ -\Delta_{\text{eq}}^{\sigma_\mu\dagger}(\mathbf{k}_F) & 0 \end{pmatrix}, \quad (14b)$$

where  $\Delta_{\text{eq}}^{\sigma_\mu}(\mathbf{k}_F)$  is the equilibrium gap function in the same sector. In the SCTMA, the equilibrium impurity self-energy is obtained simply by using the corresponding Green function in Eq. (13), so that in each spin sector,

$$\check{\sigma}_{\text{imp,eq}}^{\sigma_\mu} = -\Gamma_{\text{imp}} \left[ \cot \delta + \left\langle \frac{\check{g}_{\text{eq}}^{\sigma_\mu}}{\pi} \right\rangle_{\text{FS}} \right]^{-1}. \quad (15)$$

The solution for the equilibrium Green function is,

$$\underline{g}_{\text{eq}}^{\sigma_\mu R, A} = -\pi \frac{M^{\sigma_\mu R, A}}{D^{\sigma_\mu R, A}}, \quad (16a)$$

$$\underline{g}_{\text{eq}}^{\sigma_\mu K} = (\underline{g}_{\text{eq}}^{\sigma_\mu R} - \underline{g}_{\text{eq}}^{\sigma_\mu A}) \tanh\left(\frac{\epsilon}{2T}\right), \quad (16b)$$

where the numerator,  $M^{\sigma_\mu R, A} = \tilde{\epsilon}^{\sigma_\mu R, A} \underline{\tau}_z - \underline{\Delta}_{\text{eq}}^{\sigma_\mu}$ , and the denominator,  $D^{\sigma_\mu R, A} = \sqrt{|\Delta_{\text{eq}}^{\sigma_\mu}(\mathbf{k}_F)|^2 - \tilde{\epsilon}^{\sigma_\mu R, A}{}^2}$ , are defined with the renormalized energy,  $\tilde{\epsilon}^{\sigma_\mu R, A} = \epsilon - \frac{1}{2} \text{Tr}(\underline{\tau}_z \sigma_{\text{imp,eq}}^{\sigma_\mu R, A})$ . Note that  $\check{\sigma}_{\text{imp,eq}}^{\sigma_\mu}$  is diagonal in the particle-hole space because  $\langle \Delta_{\text{eq}}^{\sigma_\mu}(\mathbf{k}_F) \rangle_{\text{FS}} = 0$  is satisfied in spin-triplet superconductors.

The equilibrium Green function obtained above is spatially uniform. If the thermal gradient driving the system away from equilibrium results in the slow spatial dependence of the quasiparticle population, we can develop a perturbation theory for the thermal gradient. In this case, the nonequilibrium correction to the quasiclassical Green function obeys the equation,

$$\left[ \epsilon \check{\tau}_z - \check{\Delta}_{\text{eq}}^{\sigma_\mu}(\mathbf{k}_F) - \check{\sigma}_{\text{imp,eq}}^{\sigma_\mu}, \delta\check{g}^{\sigma_\mu} \right] - \left[ \delta\check{\sigma}_{\text{imp}}^{\sigma_\mu}, \check{g}_{\text{eq}}^{\sigma_\mu} \right] + i\nu_F \cdot \nabla \check{g}_{\text{eq}}^{\sigma_\mu} = 0, \quad (17)$$

which is supplemented by  $\{\check{g}_{\text{eq}}^{\sigma_\mu}, \delta\check{g}^{\sigma_\mu}\} = 0$  and the appropriate self-consistency conditions for the impurity self-energy.

We now implement this scheme for the thermal gradient. According to the discussion above, we need to make two steps. First, we assume a local equilibrium  $T = T(\mathbf{x})$  and expand the spatial gradient as  $\nabla \rightarrow \nabla T \frac{\partial}{\partial T} + \partial$ , where  $\partial$  is the spatial gradient acting on the gap function [95, 96]. Crucially, as discussed in the main text, the thermal gradient leads to changes in the pairing self-energy and we need to introduce a uniform supercurrent that maintains the Meissner state and compensates the thermoelectric quasiparticle current. Therefore, we second modify the gap function as  $\Delta_{\text{eq}}^{\sigma_\mu}(\mathbf{k}_F) \rightarrow e^{i\mathbf{Q} \cdot \mathbf{x}} \Delta_{\text{eq}}^{\sigma_\mu}(\mathbf{k}_F)$ , where  $\mathbf{Q}$  is the center of mass momentum of Cooper pairs. At this stage,  $\mathbf{Q}$  is a parameter for calculations and should be determined to satisfy  $\mathbf{J}_{\text{QP}} + \mathbf{J}_{\text{SC}} = 0$  [80]. With this change, the gradient operates on the gap function and then Eq. (17) becomes,

$$\left[ \epsilon \check{\tau}_z - \check{\Delta}_{\text{eq}}^{\sigma_\mu}(\mathbf{k}_F) - \check{\sigma}_{\text{imp,eq}}^{\sigma_\mu}, \delta\check{g}^{\sigma_\mu} \right] - \left[ \delta\check{\sigma}_{\text{imp}}^{\sigma_\mu}, \check{g}_{\text{eq}}^{\sigma_\mu} \right] + i\nu_F \cdot \nabla T \frac{\partial}{\partial T} \check{g}_{\text{eq}}^{\sigma_\mu} + i\nu_F \cdot \partial \check{g}_{\text{eq}}^{\sigma_\mu} = 0. \quad (18)$$

The third (fourth) term in Eq. (18) describes the coupling between quasiparticles (Cooper pairs) and the thermal gradient.

It is convenient to separate the nonequilibrium Green function into the quasiparticle part,  $\delta\check{g}_{\text{QP}}^{\sigma_\mu}$ , and the supercurrent part,  $\delta\check{g}_{\text{SC}}^{\sigma_\mu}$ . This separation divides Eq. (18) into,

$$\left[ \epsilon \check{\tau}_z - \check{\Delta}_{\text{eq}}^{\sigma_\mu}(\mathbf{k}_F) - \check{\sigma}_{\text{imp,eq}}^{\sigma_\mu}, \delta\check{g}_{\text{QP}}^{\sigma_\mu} \right] - \left[ \delta\check{\sigma}_{\text{imp}}^{\sigma_\mu}, \check{g}_{\text{eq}}^{\sigma_\mu} \right] + i\nu_F \cdot \nabla T \frac{\partial}{\partial T} \check{g}_{\text{eq}}^{\sigma_\mu} = 0, \quad (19)$$

$$\left[ \epsilon \check{\tau}_z - \check{\Delta}_{\text{eq}}^{\sigma_\mu}(\mathbf{k}_F) - \check{\sigma}_{\text{imp,eq}}^{\sigma_\mu}, \delta\check{g}_{\text{SC}}^{\sigma_\mu} \right] + i\nu_F \cdot \partial \check{g}_{\text{eq}}^{\sigma_\mu} = 0. \quad (20)$$

Eq. (19) (Eq. (20)) describes the responses of quasiparticles (Cooper pairs) to the thermal gradient. In Eq. (20), we set  $\delta\check{\sigma}_{\text{imp}}^{\sigma\mu} = 0$  because the supercurrent is not sensitive to impurities.

In principle,  $\delta\check{g}_{\text{QP}}^{\sigma\mu}$  and  $\delta\check{g}_{\text{SC}}^{\sigma\mu}$  are coupled with each other through the impurity self-energy and the normalization condition,  $\{\check{g}_{\text{eq}}^{\sigma\mu}, \delta\check{g}_{\text{QP}}^{\sigma\mu} + \delta\check{g}_{\text{SC}}^{\sigma\mu}\} = 0$ . However, note that if we solve Eqs. (20)-(21) assuming that the anticommutators vanish individually,  $\{\check{g}_{\text{eq}}^{\sigma\mu}, \delta\check{g}_{\text{QP}}^{\sigma\mu}\} = \{\check{g}_{\text{eq}}^{\sigma\mu}, \delta\check{g}_{\text{SC}}^{\sigma\mu}\} = 0$ , the resulting equation for the correction to the quasiclassical Green function,  $\delta\eta = \delta\check{g}^{\sigma\mu} - \check{g}_{\text{QP}}^{\sigma\mu} - \check{g}_{\text{SC}}^{\sigma\mu}$ , does not involve ‘‘driving terms’’ proportional to the thermal gradient. It follows that in the linear response regime, the coupling between  $\delta\check{g}_{\text{QP}}^{\sigma\mu}$  and  $\delta\check{g}_{\text{SC}}^{\sigma\mu}$  introduces corrections only to nonlinear transport. Hence, we neglect it in our calculations. In the same approximation, the nonequilibrium part of the impurity self-energy is additive for the two components of quasiparticle and Cooper pairs and also satisfies the normalization condition (see Eq. (27) below).

### Nonequilibrium quasiclassical Green function

On the basis of the theoretical framework presented above, we derive the nonequilibrium quasiclassical Green function. We first derive the expression for the quasiparticle contribution,  $\delta\check{g}_{\text{QP}}^{\sigma\mu X}$  ( $X = \text{R}, \text{A}$ ), using Eq. (19), which now reads,

$$\left[ \underline{M}^{\sigma\mu X}, \delta\check{g}_{\text{QP}}^{\sigma\mu X} \right] - \left[ \delta\check{\sigma}_{\text{imp}}^{\sigma\mu X}, \check{g}_{\text{eq}}^{\sigma\mu X} \right] + i\nu_{\text{F}} \cdot \nabla T \frac{\partial}{\partial T} \check{g}_{\text{eq}}^{\sigma\mu X} = 0. \quad (21)$$

Using the constraint  $\{\check{g}_{\text{eq}}^{\sigma\mu X}, \delta\check{g}_{\text{QP}}^{\sigma\mu X}\} = 0$  ( $X = \text{R}, \text{A}$ ), we obtain,

$$\delta\check{g}_{\text{QP}}^{\sigma\mu X} = \frac{\check{g}_{\text{eq}}^{\sigma\mu X}}{2\pi D^{\sigma\mu X}} \left( \left[ \delta\check{\sigma}_{\text{imp}}^{\sigma\mu X}, \check{g}_{\text{eq}}^{\sigma\mu X} \right] - i\nu_{\text{F}} \cdot \nabla T \frac{\partial}{\partial T} \check{g}_{\text{eq}}^{\sigma\mu X} \right). \quad (22)$$

We now turn to the Keldysh component,  $\delta\check{g}_{\text{QP}}^{\sigma\mu \text{K}}$ . Writing the corresponding matrix components of Eq. (19), we have,

$$\begin{aligned} & \left( \underline{M}^{\sigma\mu \text{R}} \delta\check{g}_{\text{QP}}^{\sigma\mu \text{K}} - \delta\check{g}_{\text{QP}}^{\sigma\mu \text{K}} \underline{M}^{\sigma\mu \text{A}} \right) - \left( \sigma_{\text{imp,eq0}}^{\sigma\mu \text{R}} - \sigma_{\text{imp,eq0}}^{\sigma\mu \text{A}} \right) \delta\check{g}_{\text{QP}}^{\sigma\mu \text{K}} \\ & + \left( \delta\check{g}_{\text{QP}}^{\sigma\mu \text{R}} \sigma_{\text{imp,eq}}^{\sigma\mu \text{K}} - \sigma_{\text{imp,eq}}^{\sigma\mu \text{K}} \delta\check{g}_{\text{QP}}^{\sigma\mu \text{A}} \right) \\ & - \left( \delta\check{\sigma}_{\text{imp}}^{\sigma\mu \text{R}} \check{g}_{\text{eq}}^{\sigma\mu \text{K}} - \check{g}_{\text{eq}}^{\sigma\mu \text{K}} \delta\check{\sigma}_{\text{imp}}^{\sigma\mu \text{A}} \right) - \left( \delta\check{\sigma}_{\text{imp}}^{\sigma\mu \text{K}} \check{g}_{\text{eq}}^{\sigma\mu \text{A}} - \check{g}_{\text{eq}}^{\sigma\mu \text{R}} \delta\check{\sigma}_{\text{imp}}^{\sigma\mu \text{K}} \right) \\ & + i\nu_{\text{F}} \cdot \nabla T \frac{\partial}{\partial T} \check{g}_{\text{eq}}^{\sigma\mu \text{K}} = 0, \end{aligned} \quad (23)$$

which is supplemented by  $\check{g}_{\text{eq}}^{\sigma\mu \text{R}} \delta\check{g}_{\text{QP}}^{\sigma\mu \text{K}} + \delta\check{g}_{\text{QP}}^{\sigma\mu \text{K}} \check{g}_{\text{eq}}^{\sigma\mu \text{A}} = 0$ . Here, we defined for brevity  $\sigma_{\text{imp,eq0}}^{\sigma\mu \text{R,A}} = \text{Tr}(\sigma_{\text{imp,eq0}}^{\sigma\mu \text{R,A}})$ . To simplify Eq. (23), let us write  $\delta\check{g}_{\text{QP}}^{\sigma\mu \text{K}}$  and  $\delta\check{\sigma}_{\text{imp}}^{\sigma\mu \text{K}}$  as [97],

$$\delta\check{g}_{\text{QP}}^{\sigma\mu \text{K}} = \left( \delta\check{g}_{\text{QP}}^{\sigma\mu \text{R}} - \delta\check{g}_{\text{QP}}^{\sigma\mu \text{A}} \right) \tanh\left(\frac{\epsilon}{2T}\right) + \delta\check{g}_{\text{QP}}^{\sigma\mu \text{a}}, \quad (24)$$

$$\delta\check{\sigma}_{\text{imp}}^{\sigma\mu \text{K}} = \left( \delta\check{\sigma}_{\text{imp}}^{\sigma\mu \text{R}} - \delta\check{\sigma}_{\text{imp}}^{\sigma\mu \text{A}} \right) \tanh\left(\frac{\epsilon}{2T}\right) + \delta\check{\sigma}_{\text{imp}}^{\sigma\mu \text{a}}. \quad (25)$$

The first term in Eq. (24) describes the changes in the spectral function while maintaining the distribution function in equilibrium. The second term in Eq. (24) describes the changes in the distribution function and is essential for the response to the thermal gradient. Using Eq. (24) and Eq. (25), we recast Eq. (23) as,

$$\begin{aligned} & \left( \underline{M}^{\sigma\mu \text{R}} \delta\check{g}_{\text{QP}}^{\sigma\mu \text{a}} - \delta\check{g}_{\text{QP}}^{\sigma\mu \text{a}} \underline{M}^{\sigma\mu \text{A}} \right) - \left( \sigma_{\text{imp,eq0}}^{\sigma\mu \text{R}} - \sigma_{\text{imp,eq0}}^{\sigma\mu \text{A}} \right) \delta\check{g}_{\text{QP}}^{\sigma\mu \text{a}} \\ & + \left( \check{g}_{\text{eq}}^{\sigma\mu \text{R}} \delta\check{\sigma}_{\text{imp}}^{\sigma\mu \text{a}} - \delta\check{\sigma}_{\text{imp}}^{\sigma\mu \text{a}} \check{g}_{\text{eq}}^{\sigma\mu \text{A}} \right) \\ & - \frac{i\epsilon\nu_{\text{F}} \cdot \nabla T}{2T^2 \cosh^2\left(\frac{\epsilon}{2T}\right)} \left( \check{g}_{\text{eq}}^{\sigma\mu \text{R}} - \check{g}_{\text{eq}}^{\sigma\mu \text{A}} \right) = 0. \end{aligned} \quad (26)$$

The corresponding constraint from the normalization condition on  $\delta\check{g}_{\text{QP}}^{\sigma\mu \text{a}}$  becomes  $\check{g}_{\text{eq}}^{\sigma\mu \text{R}} \delta\check{g}_{\text{QP}}^{\sigma\mu \text{a}} + \delta\check{g}_{\text{QP}}^{\sigma\mu \text{a}} \check{g}_{\text{eq}}^{\sigma\mu \text{A}} = 0$ . Using Eq. (24) and Eq. (25), we obtain the  $T$ -matrix equation for  $\delta\check{\sigma}_{\text{imp}}^{\sigma\mu \text{a}}$ ,

$$\begin{aligned} \delta\check{\sigma}_{\text{imp}}^{\sigma\mu \text{a}} = & -\Gamma_{\text{imp}} \left( \cot\delta + \left\langle \frac{\check{g}_{\text{eq}}^{\sigma\mu \text{R}}}{\pi} \right\rangle_{\text{FS}} \right)^{-1} \\ & \times \left\langle \frac{\delta\check{g}_{\text{QP}}^{\sigma\mu \text{a}}}{\pi} \right\rangle_{\text{FS}} \left( \cot\delta + \left\langle \frac{\check{g}_{\text{eq}}^{\sigma\mu \text{A}}}{\pi} \right\rangle_{\text{FS}} \right)^{-1}. \end{aligned} \quad (27)$$

Using  $\check{g}_{\text{eq}}^{\sigma\mu \text{R}} \delta\check{g}_{\text{QP}}^{\sigma\mu \text{a}} + \delta\check{g}_{\text{QP}}^{\sigma\mu \text{a}} \check{g}_{\text{eq}}^{\sigma\mu \text{A}} = 0$ , we obtain,

$$\delta\check{g}_{\text{QP}}^{\sigma\mu \text{a}} = \delta\check{g}_{\text{ns}}^{\sigma\mu \text{a}} + \delta\check{g}_{\text{vc}}^{\sigma\mu \text{a}}, \quad (28a)$$

$$\delta\check{g}_{\text{ns}}^{\sigma\mu \text{a}} = \underline{N}_{\text{eq}}^{\sigma\mu \text{R}} \left( \check{g}_{\text{eq}}^{\sigma\mu \text{R}} - \check{g}_{\text{eq}}^{\sigma\mu \text{A}} \right) \left( \frac{-i\epsilon\nu_{\text{F}} \cdot \nabla T}{2T^2 \cosh^2\left(\frac{\epsilon}{2T}\right)} \right) \quad (28b)$$

$$\delta\check{g}_{\text{vc}}^{\sigma\mu \text{a}} = \underline{N}_{\text{eq}}^{\sigma\mu \text{R}} \left( \check{g}_{\text{eq}}^{\sigma\mu \text{R}} \delta\check{\sigma}_{\text{imp}}^{\sigma\mu \text{a}} - \delta\check{\sigma}_{\text{imp}}^{\sigma\mu \text{a}} \check{g}_{\text{eq}}^{\sigma\mu \text{A}} \right), \quad (28c)$$

where

$$\underline{N}_{\text{eq}}^{\sigma\mu \text{R}} = \frac{-(D^{\sigma\mu \text{R}} + D^{\sigma\mu \text{A}}) \frac{\check{g}_{\text{eq}}^{\sigma\mu \text{R}}}{\pi} + \sigma_{\text{imp,eq0}}^{\sigma\mu \text{R}} - \sigma_{\text{imp,eq0}}^{\sigma\mu \text{A}}}{(D^{\sigma\mu \text{R}} - D^{\sigma\mu \text{A}})^2 + \left( \sigma_{\text{imp,eq0}}^{\sigma\mu \text{R}} - \sigma_{\text{imp,eq0}}^{\sigma\mu \text{A}} \right)^2}. \quad (29)$$

The first term in Eq. (28a) only depends on the impurity self-energy in equilibrium. This term describes the ‘‘bare bubble’’: the spin current and the thermal-current vertices connected by the two equilibrium Green functions in the diagrammatic calculations. The second term involves the impurity self-energy in the nonequilibrium state and accounts for the vertex corrections [72–74]. Indeed, expanding Eq. (27), we find terms coexisting of both the advanced and retarded Green functions, such as  $\epsilon\nu_{\text{F}} \check{g}_{\text{eq}}^{\sigma\mu \text{R}} \delta\check{g}_{\text{QP}}^{\sigma\mu \text{a}}$ . Thus,  $\delta\check{\sigma}_{\text{imp}}^{\sigma\mu \text{a}}$  contains the vertex corrections to the thermal-current [98]. This second term is more essential for the SSE and the SNE because the anisotropy between the electron and hole propagators appears through the impurity vertex corrections [27].

We finally consider  $\delta\check{g}_{\text{SC}}^{\sigma\mu}$  using Eq. (20), which takes the form

$$\left[ \underline{M}^{\sigma\mu \text{R,A}}, \delta\check{g}_{\text{SC}}^{\sigma\mu \text{R,A}} \right] + i\nu_{\text{F}} \cdot \partial \check{g}_{\text{eq}}^{\sigma\mu \text{R,A}} = 0. \quad (30)$$

Using the normalization constraint,  $\{g_{\text{eq}}^{\sigma_\mu R,A}, \delta g_{\text{SC}}^{\sigma_\mu R,A}\} = 0$ , we obtain,

$$\delta g_{\text{SC}}^{\sigma_\mu R,A} = -\frac{(\mathbf{v}_F \cdot \mathbf{Q}) g_{\text{eq}}^{\sigma_\mu R,A} \tau_y \Delta_{\text{eq}}^{\sigma_\mu}}{2D\sigma_\mu R,A^2}, \quad (31a)$$

$$\delta g_{\text{SC}}^{\sigma_\mu K} = (\delta g_{\text{SC}}^{\sigma_\mu R} - \delta g_{\text{SC}}^{\sigma_\mu A}) \tanh\left(\frac{\epsilon}{2T}\right). \quad (31b)$$

We now have the nonequilibrium Green functions necessary to compute the spin current.

### Spin current response to the thermal gradient

In spin-triplet superconductors, both quasiparticles and Cooper pairs carry the spin and electric currents. Using Eq. (22) and Eq. (28a), the spin and electric currents carried by the quasiparticles are expressed via the Green functions as [27],

$$\mathbf{J}_{\text{QP}}^{\sigma_\mu} = \frac{N(\epsilon_F)}{2} \sum_{\sigma_\mu=\pm 1} \int \frac{d\epsilon}{4\pi i} \left\langle \text{Tr} \left[ \mathbf{v}_F \sigma_\mu \tau_z \delta g_{\text{QP}}^{\sigma_\mu K} \right] \right\rangle_{\text{FS}} \quad (32a)$$

$$\mathbf{J}_{\text{QP}} = \frac{N(\epsilon_F)}{2} \sum_{\sigma_\mu=\pm 1} \int \frac{d\epsilon}{4\pi i} \left\langle \text{Tr} \left[ \mathbf{v}_F \tau_z \delta g_{\text{QP}}^{\sigma_\mu K} \right] \right\rangle_{\text{FS}}. \quad (32b)$$

Using Eqs. (31) the spin and electric supercurrents are expressed as,

$$\mathbf{J}_{\text{SC}}^{\sigma_\mu} = \frac{N(\epsilon_F)}{2} \sum_{\sigma_\mu=\pm 1} \int \frac{d\epsilon}{4\pi i} \left\langle \text{Tr} \left[ \mathbf{v}_F \sigma_\mu \tau_z \delta g_{\text{SC}}^{\sigma_\mu K} \right] \right\rangle_{\text{FS}} \quad (33a)$$

$$\mathbf{J}_{\text{SC}} = \frac{N(\epsilon_F)}{2} \sum_{\sigma_\mu=\pm 1} \int \frac{d\epsilon}{4\pi i} \left\langle \text{Tr} \left[ \mathbf{v}_F \tau_z \delta g_{\text{SC}}^{\sigma_\mu K} \right] \right\rangle_{\text{FS}}. \quad (33b)$$

We now determine the phase gradient,  $\mathbf{Q}$ , such that the thermoelectric current vanishes,  $\mathbf{J}_{\text{QP}} + \mathbf{J}_{\text{SC}} = 0$  [80]. Using Eq. (32b) and Eq. (33b), this condition is expressed as,

$$\sum_{\sigma_\mu=\pm 1} \int \frac{d\epsilon}{4\pi i} \left\langle \text{Tr} \left[ \mathbf{v}_F \sigma_\mu \tau_z \left( \delta g_{\text{QP}}^{\sigma_\mu K} + \delta g_{\text{SC}}^{\sigma_\mu K} \right) \right] \right\rangle_{\text{FS}} = 0. \quad (34)$$

We solve Eq. (34) for  $\mathbf{Q}$ , and then compute the spin current,  $\mathbf{J}^{\sigma_\mu} = \mathbf{J}_{\text{QP}}^{\sigma_\mu} + \mathbf{J}_{\text{SC}}^{\sigma_\mu}$ , driven by the thermal gradient.

### Acknowledgement

T. Matsushita thanks M. Sato, Y. Yanase, T. Shibauchi, K. Hashimoto, K. Ishihara and J. Fujimoto, J. Tei for fruitful discussions.

### Funding

T. Matsushita was supported by a Japan Society for the Promotion of Science (JSPS) Fellowship for Young Scientists,

JSPS KAKENHI Grant No. JP19J20144, and JST CREST Grant No. JPMJCR19T2. I. V. was supported in part by grant NSF PHY-1748958 to the Kavli Institute for Theoretical Physics (KITP). This work was also supported by JST CREST Grant No. JPMJCR19T5, Japan, and the Grant-in-Aid for Scientific Research on Innovative Areas ‘‘Quantum Liquid Crystals (JP22H04480)’’ from JSPS of Japan, and JSPS KAKENHI (Grants No. JP20K03860, No. JP21H01039, and No. JP22H01221).

### Availability

T. Matsushita and I. Vekhter conceived this work and constructed the linear response theory to the thermal gradient. T. Matsushita and T. Mizushima performed the symmetry-based analysis for the SSE and the SNE. All authors discussed the calculated results and wrote the paper.

### Competing interests

The authors declare that they have no competing interests.

### Availability

All data needed to evaluate the conclusions in the paper are presented in the paper. Additional data related to this paper may be requested from the authors.

- [1] M. Sigrist and K. Ueda, *Phenomenological theory of unconventional superconductivity*, Rev. of Mod. Phys. **63**, 239 (1991).
- [2] J. F. Annett, *Symmetry of the order parameter for high-temperature superconductivity*, Adv. Phys. **39**, 83 (1990).
- [3] G. E. Volovik and L. P. Gor'kov, *Superconducting classes in heavy-fermion systems*, Sov. Phys JETP **61**, 843 (1985).
- [4] X.-L. Qi and S.-C. Zhang, *Topological insulators and superconductors*, Rev. Mod. Phys. **83**, 1057 (2011).
- [5] M. Sato and S. Fujimoto, *Majorana fermions and topology in superconductors*, J. Phys. Soc. Jpn **85**, 072001 (2016).
- [6] M. Sato and Y. Ando, *Topological superconductors: a review*, Rep. Prog. Phys. **80**, 076501 (2017).
- [7] A. Buzdin and A. Koshelev, *Periodic alternating 0- and  $\pi$ -junction structures as realization of  $\varphi$ -Josephson junctions*, Phys. Rev. B **67**, 220504 (2003).
- [8] I. Margaris, V. Paltoglou, and N. Flytzanis, *Zero phase difference supercurrent in ferromagnetic Josephson junctions*, J. Phys.: Condens. Matter **22**, 445701 (2010).
- [9] A. Buzdin, *Direct coupling between magnetism and superconducting current in the Josephson  $\varphi_0$  junction*, Phys. Rev. Lett. **101**, 107005 (2008).
- [10] I. Kulagina and J. Linder, *Spin supercurrent, magnetization dynamics, and  $\varphi$ -state in spin-textured Josephson junctions*, Phys. Rev. B **90**, 054504 (2014).

- [11] P. D. Sacramento, L. C. F. Silva, G. S. Nunes, M. A. N. Araújo, and V. R. Vieira, *Supercurrent-induced domain wall motion*, Phys. Rev. B **83**, 054403 (2011).
- [12] P. D. Sacramento and M. A. N. Araújo, *Spin torque on magnetic domain walls exerted by supercurrents*, Eur. Phys. J. B **76**, 251 (2010).
- [13] R. Takashima, S. Fujimoto, and T. Yokoyama, *Adiabatic and nonadiabatic spin torques induced by a spin-triplet supercurrent*, Phys. Rev. B **96**, 121203 (2017).
- [14] J. Linder and K. Halterman, *Superconducting spintronics with magnetic domain walls*, Phys. Rev. B **90**, 104502 (2014).
- [15] F. S. Bergeret, A. F. Volkov, and K. B. Efetov, *Long-range proximity effects in superconductor-ferromagnet structures*, Physical Rev. Lett. **86**, 4096 (2001).
- [16] A. Kadigrobov, R. I. Shekhter, and M. Jonson, *Quantum spin fluctuations as a source of long-range proximity effects in diffusive ferromagnet-superconductor structures*, EPL **54**, 394 (2001).
- [17] F. S. Bergeret, A. F. Volkov, and K. B. Efetov, *Odd triplet superconductivity and related phenomena in superconductor-ferromagnet structures*, Rev. Mod. Phys. **77**, 1321 (2005).
- [18] A. F. Volkov, F. S. Bergeret, and K. B. Efetov, *Odd triplet superconductivity in superconductor-ferromagnet multilayered structures*, Physical Rev. Lett. **90**, 117006 (2003).
- [19] M. Eschrig, J. Kopu, J. C. Cuevas, and G. Schön, *Theory of half-metal/superconductor heterostructures*, Phys. Rev. Lett. **90**, 137003 (2003).
- [20] K. Uchida, *Transport phenomena in spin caloritronics*, Proc. Japan Acad. Ser. B **97**, 69 (2021).
- [21] K. Uchida, S. Takahashi, K. Harii, J. Ieda, W. Koshibae, K. Ando, S. Maekawa, and E. Saitoh, *Observation of the spin Seebeck effect*, Nature **455**, 778 (2008).
- [22] K. Uchida, J. Xiao, H. Adachi, J. Ohe, S. Takahashi, J. Ieda, T. Ota, Y. Kajiwara, H. Umezawa, H. Kawai, G. E. W. Bauer, S. Maekawa, and E. Saitoh, *Spin Seebeck Insulator*, Nat. Mater. **9**, 894 (2010).
- [23] C. M. Jaworski, J. Yang, S. Mack, D. D. Awschalom, J. P. Heremans, and R. C. Myers, *Observation of the spin-Seebeck effect in a ferromagnetic semiconductor*, Nat. Mater. **9**, 898 (2010).
- [24] S. Bosu, Y. Sakuraba, K. Uchida, K. Saito, T. Ota, E. Saitoh, and K. Takanashi, *Spin Seebeck effect in thin films of the Heusler compound  $\text{Co}_2\text{MnSi}$* , Phys. Rev. B **83**, 224401 (2011).
- [25] S. Meyer, Y. T. Chen, S. Wimmer, M. Althammer, T. Wimmer, R. Schlitz, S. Geprägs, H. Huebl, D. Ködderitzsch, H. Ebert, G. E. W. Bauer, R. Gross, and S. T. B. Goennenwein, *Observation of the spin Nernst effect*, Nat. Mater. **16**, 977 (2017).
- [26] P. Sheng, Y. Sakuraba, Y.-C. Lau, S. Takahashi, S. Mitani, and M. Hayashi, *The spin Nernst effect in tungsten*, Sci. Adv. **3**, e1701503 (2017).
- [27] T. Matsushita, J. Ando, Y. Masaki, T. Mizushima, S. Fujimoto, and I. Vekhter, *Spin-Nernst Effect in Time-Reversal-Invariant Topological Superconductors*, Phys. Rev. Lett. **128**, 097001 (2022).
- [28] G. Eilenberger, *Transformation of Gorkov's equation for type II superconductors into transport-like equations*, Z. Physik **214**, 195 (1968).
- [29] J. Serene and D. Rainer, *The quasiclassical approach to superfluid  $^3\text{He}$* , Phys. Rep. **101**, 221 (1983).
- [30] M. Tinkham, *Introduction to Superconductivity* (Dover Publications, 2004).
- [31] D. Vollhardt and P. Wolfe, *The Superfluid Phases of Helium 3* (Courier Corporation, 2013).
- [32] H. Kojima and H. Ishimoto, *Spin Polarized Superfluid  $^3\text{He A1}$* , J. Phys. Soc. Jpn. **77**, 111001 (2008).
- [33] H. R. Ott, H. Rudigier, Z. Fisk, and J. L. Smith, *Phase transition in the superconducting state of  $\text{U}_{1-x}\text{Th}_x\text{Be}_{13}$  ( $x = 0 - 0.06$ )*, Phys. Rev. B **31**, 1651 (1985).
- [34] J. S. Kim, B. Andraka, and G. R. Stewart, *Investigation of the second transition in  $\text{U}_{1-x}\text{Th}_x\text{Be}_{13}$* , Phys. Rev. B **44**, 6921 (1991).
- [35] Y. Shimizu, S. Kittaka, S. Nakamura, T. Sakakibara, D. Aoki, Y. Homma, A. Nakamura, and K. Machida, *Quasiparticle excitations and evidence for superconducting double transitions in monocrystalline  $\text{U}_{0.97}\text{Th}_{0.03}\text{Be}_{13}$* , Phys. Rev. B **96**, 100505 (2017).
- [36] R. H. Heffner, J. L. Smith, J. O. Willis, P. Birrer, C. Baines, F. N. Gygax, B. Hitti, E. Lippelt, H. R. Ott, A. Schenck, E. A. Knetsch, J. A. Mydosh, and D. E. MacLaughlin, *New phase diagram for  $(\text{U, Th})\text{Be}_{13}$ : A muon-spin-resonance and  $\text{H}_{\text{C1}}$  study*, Phys. Rev. Lett. **65**, 2816 (1990).
- [37] B. Batlogg, D. Bishop, B. Golding, C. M. Varma, Z. Fisk, J. L. Smith, and H. R. Ott,  *$\lambda$ -Shaped Ultrasound-Attenuation Peak in Superconducting  $(\text{U, Th})\text{Be}_{13}$* , Phys. Rev. Lett. **55**, 1319 (1985).
- [38] D. S. Jin, T. F. Rosenbaum, J. S. Kim, and G. R. Stewart, *Low-temperature specific heat of  $\text{U}_{1-x}\text{Th}_x\text{Be}_{13}$* , Phys. Rev. B **49**, 1540 (1994).
- [39] K. Machida, *Spin Triplet Nematic Pairing Symmetry and Superconducting Double Transition in  $\text{U}_{1-x}\text{Th}_x\text{Be}_{13}$* , J. Phys. Soc. Jpn. **87**, 033703 (2018).
- [40] T. Mizushima and M. Nitta, *Topology and symmetry of surface Majorana arcs in cyclic superconductors*, Phys. Rev. B **97**, 024506 (2018).
- [41] L. Jiao, S. Howard, S. Ran, Z. Wang, J. O. Rodriguez, M. Sgrist, Z. Wang, N. P. Butch, and V. Madhavan, *Chiral superconductivity in heavy-fermion metal  $\text{UTe}_2$* , Nature **579**, 523 (2020).
- [42] I. M. Hayes, D. S. Wei, T. Metz, J. Zhang, Y. S. Eo, S. Ran, S. R. Saha, J. Collini, N. P. Butch, D. F. Agterberg, A. Kapitulnik, and J. Paglione, *Multicomponent superconducting order parameter in  $\text{UTe}_2$* , Science **373**, 797 (2021).
- [43] K. Ishihara, M. Roppongi, M. Kobayashi, K. Imamura, Y. Mizukami, H. Sakai, P. Opletal, Y. Tokiwa, Y. Haga, K. Hashimoto, and T. Shibauchi, *Chiral superconductivity in  $\text{UTe}_2$  probed by anisotropic low-energy excitations*, Nat. Commun. **14**, 2966 (2023).
- [44] D. Aoki, K. Ishida, and J. Flouquet, *Review of U-based Ferromagnetic Superconductors: Comparison between  $\text{UGe}_2$ ,  $\text{URhGe}$ , and  $\text{UCoGe}$* , J. Phys. Soc. Jpn. **88**, 022001 (2019).
- [45] V. Mineev, *Superconducting states in ferromagnetic metals*, Phys. Rev. B **66**, 134504 (2002).
- [46] T. Hattori, Y. Ihara, Y. Nakai, K. Ishida, Y. Tada, S. Fujimoto, N. Kawakami, E. Osaki, K. Deguchi, N. K. Sato, and I. Satoh, *Superconductivity Induced by Longitudinal Ferromagnetic Fluctuations in  $\text{UCoGe}$* , Phys. Rev. Lett. **108**, 066403 (2012).
- [47] M. Seemann, D. Ködderitzsch, S. Wimmer, and H. Ebert, *Symmetry-imposed shape of linear response tensors*, Phys. Rev. B **92**, 155138 (2015).
- [48] S. Wimmer, M. Seemann, K. Chadova, D. Ködderitzsch, and H. Ebert, *Spin-orbit-induced longitudinal spin-polarized currents in nonmagnetic solids*, Phys. Rev. B **92**, 041101 (2015).
- [49] C. Kallin, *Chiral p-wave order in  $\text{Sr}_2\text{RuO}_4$* , Rep. Prog. Phys. **75**, 042501 (2012).
- [50] S. Kittaka, Y. Shimizu, T. Sakakibara, Y. Haga, E. Yamamoto, Y. Ōnuki, Y. Tsutsumi, T. Nomoto, H. Ikeda, and K. Machida, *Evidence for chiral d-wave superconductivity in  $\text{URu}_2\text{Si}_2$  from the field-angle variation of its specific heat*, J. Phys. Soc. Jpn. **85**, 033704 (2016).

- [51] T. Yamashita, Y. Shimoyama, Y. Haga, T. D. Matsuda, E. Yamamoto, Y. Onuki, H. Sumiyoshi, S. Fujimoto, A. Levchenko, T. Shibauchi, and Y. Matsuda, *Colossal thermomagnetic response in the exotic superconductor URu<sub>2</sub>Si<sub>2</sub>*, Nat. Phys. **11**, 17 (2015).
- [52] H. Sumiyoshi and S. Fujimoto, *Giant Nernst and Hall effects due to chiral superconducting fluctuations*, Phys. Rev. B **90**, 184518 (2014).
- [53] P. K. Biswas, H. Luetkens, T. Neupert, T. Stürzer, C. Baines, G. Pascua, A. P. Schnyder, M. H. Fischer, J. Goryo, M. R. Lees, H. Maeter, F. Brückner, H.-H. Klauss, M. Nicklas, P. J. Baker, A. D. Hillier, M. Sigrist, A. Amato, and D. Johrendt, *Evidence for superconductivity with broken time-reversal symmetry in locally noncentrosymmetric SrPtAs*, Phys. Rev. B **87**, 180503 (2013).
- [54] H. Ueki, R. Tamura, and J. Goryo, *Possibility of chiral d-wave state in the hexagonal pnictide superconductor SrPtAs*, Phys. Rev. B **99**, 144510 (2019).
- [55] E. R. Schemm, W. J. Gannon, C. M. Wishne, W. P. Halperin, and A. Kapitulnik, *Observation of broken time-reversal symmetry in the heavy-fermion superconductor UPt<sub>3</sub>*, Science **345**, 190 (2014).
- [56] S. Yonezawa, *Nematic Superconductivity in Doped Bi<sub>2</sub>Se<sub>3</sub> Topological Superconductors*, Condens. Matter **4**, 2 (2018).
- [57] Y. Shimizu, S. Kittaka, S. Nakamura, T. Sakakibara, D. Aoki, Y. Homma, A. Nakamura, and K. Machida, *Quasiparticle excitations and evidence for superconducting double transitions in monocrystalline U<sub>0.97</sub>Th<sub>0.03</sub>Be<sub>13</sub>*, Phys. Rev. B **96**, 100505 (2017).
- [58] M. Sigrist and T. M. Rice, *Phenomenological theory of the superconductivity phase diagram of U<sub>1-x</sub>Th<sub>x</sub>Be<sub>13</sub>*, Phys. Rev. B **39**, 2200 (1989).
- [59] S. Ran, C. Eckberg, Q.-P. Ding, Y. Furukawa, T. Metz, S. R. Saha, I.-L. Liu, M. Zic, H. Kim, J. Paglione, and N. P. Butch, *Nearly ferromagnetic spin-triplet superconductivity*, Science **365**, 684 (2019).
- [60] G. Knebel, W. Knafo, A. Pourret, Q. Niu, M. Vališka, D. Braithwaite, G. Lapertot, M. Nardone, A. Zitouni, S. Mishra, I. Sheikin, G. Seyfarth, J.-P. Brison, D. Aoki, and J. Flouquet, *Field-Reentrant Superconductivity Close to a Metamagnetic Transition in the Heavy-Fermion Superconductor UTe<sub>2</sub>*, J. Phys. Soc. Jpn. **88**, 063707 (2019).
- [61] J. Ishizuka, S. Sumita, A. Daido, and Y. Yanase, *Insulator-Metal Transition and Topological Superconductivity in UTe<sub>2</sub> from a First-Principles Calculation*, Phys. Rev. Lett. **123**, 217001 (2019).
- [62] J. Ishizuka and Y. Yanase, *Periodic Anderson model for magnetism and superconductivity in UTe<sub>2</sub>*, Phys. Rev. B **103**, 094504 (2021).
- [63] C. Kallin and J. Berlinsky, *Chiral superconductors*, Rep. Prog. Phys. **79**, 054502 (2016).
- [64] S. K. Ghosh, M. Smidman, T. Shang, J. F. Annett, A. D. Hillier, J. Quintanilla, and H. Yuan, *Recent progress on superconductors with time-reversal symmetry breaking*, J. Phys.: Condens. Matter **33**, 033001 (2020).
- [65] J. Goryo, *Impurity-induced polar Kerr effect in a chiral p-wave superconductor*, Phys. Rev. B **78**, 060501 (2008).
- [66] E. J. König and A. Levchenko, *Kerr Effect from Diffractive Skew Scattering in Chiral  $p_x \pm ip_y$  Superconductors*, Phys. Rev. Lett. **118**, 027001 (2017).
- [67] N. Read and D. Green, *Paired states of fermions in two dimensions with breaking of parity and time-reversal symmetries and the fractional quantum Hall effect*, Phys. Rev. B **61**, 10267 (2000).
- [68] K. Nomura, S. Ryu, A. Furusaki, and N. Nagaosa, *Cross-Correlated Responses of Topological Superconductors and Superfluids*, Phys. Rev. Lett. **108**, 026802 (2012).
- [69] H. Sumiyoshi and S. Fujimoto, *Quantum Thermal Hall effect in a Time-Reversal-Symmetry-Broken Topological Superconductor in Two Dimensions: Approach from Bulk Calculations*, J. Phys. Soc. Jpn **82**, 023602 (2013).
- [70] Y. Moriya, T. Matsushita, M. G. Yamada, T. Mizushima, and S. Fujimoto, *Intrinsic Anomalous Thermal Hall Effect in the Unconventional Superconductor UTe<sub>2</sub>*, J. Phys. Soc. Jpn. **91**, 094710 (2022).
- [71] B. Arfi, H. Bahlouli, and C. J. Pethick, *Transport properties of anisotropic superconductors: Influence of arbitrary electron-impurity phase shifts*, Phys. Rev. B **39**, 8959 (1989).
- [72] S. Yip, *Low temperature thermal hall conductivity of a nodal chiral superconductor*, Supercond. Sci. and Technol. **29**, 085006 (2016).
- [73] F. Yilmaz and S. K. Yip, *Spontaneous thermal Hall conductance in superconductors with broken time-reversal symmetry*, Phys. Rev. Res. **2**, 023223 (2020).
- [74] V. Ngampruetikorn and J. A. Sauls, *Impurity-Induced Anomalous Thermal Hall Effect in Chiral Superconductors*, Phys. Rev. Lett. **124**, 157002 (2020).
- [75] T. Matsushita, T. Mizushima, I. Vekhter, and S. Fujimoto, *Anomalous acoustoelectric effect induced by clapping modes in chiral superconductors*, Phys. Rev. B **105**, 134520 (2022).
- [76] H. Ikegami, Y. Tsutsumi, and K. Kono, *Chiral Symmetry Breaking in Superfluid <sup>3</sup>He-A*, Science **341**, 59 (2013).
- [77] H. Ikegami, Y. Tsutsumi, and K. Kono, *Observation of Intrinsic Magnus Force and Direct Detection of Chirality in Superfluid <sup>3</sup>He-A*, J. Phys. Soc. Jpn. **84**, 044602 (2015).
- [78] O. Shevtsov and J. A. Sauls, *Electron bubbles and Weyl fermions in chiral superfluid <sup>3</sup>He-A*, Phys. Rev. B **94**, 064511 (2016).
- [79] D. Einzel, *Analytic Two-Fluid Description of Unconventional Superconductivity*, J. Low Temp. Phys. **131**, 1 (2003).
- [80] V. L. Ginzburg and G. F. Zharkov, *Thermoelectric effects in superconductors*, Sov. Phys. Usp. **21**, 381 (1978).
- [81] C. D. Shelly, E. A. Matrozoza, and V. T. Petrashov, *Resolving thermoelectric “paradox” in superconductors*, Sci. Adv. **2**, e1501250 (2016).
- [82] W. P. Halperin, H. Choi, J. P. Davis, and J. Pollanen, *Impurity Effects of Aerogel in Superfluid <sup>3</sup>He*, J. Phys. Soc. Jpn. **77**, 111002 (2008).
- [83] E. V. Thuneberg, S. K. Yip, M. Fogelström, and J. A. Sauls, *Models for Superfluid <sup>3</sup>He in Aerogel*, Phys. Rev. Lett. **80**, 2861 (1998).
- [84] H. C. Choi, A. J. Gray, C. L. Vicente, J. S. Xia, G. Gervais, W. P. Halperin, N. Mulders, and Y. Lee, *A<sub>1</sub> and A<sub>2</sub> Transitions in Superfluid <sup>3</sup>He in 98% Porosity Aerogel*, Phys. Rev. Lett. **93**, 145302 (2004).
- [85] T. Ohta, T. Hattori, K. Ishida, Y. Nakai, E. Osaki, K. Deguchi, N. K. Sato, and I. Satoh, *Microscopic Coexistence of Ferromagnetism and Superconductivity in Single-Crystal UCoGe*, J. Phys. Soc. Jpn. **79**, 023707 (2010).
- [86] H. Kusunose and Y. Kimoto, *Theory of Self-Induced Vortex State in Ferromagnetic Superconductors*, J. Phys. Soc. Jpn. **82**, 094711 (2013).
- [87] M. O. Ajeesh, M. Bordelon, C. Girod, S. Mishra, F. Ronning, E. D. Bauer, B. Maiorov, J. D. Thompson, P. F. S. Rosa, and S. M. Thomas, *Fate of Time-Reversal Symmetry Breaking in UTe<sub>2</sub>*, Phys. Rev. X **13**, 041019 (2023).
- [88] J. Tei, T. Mizushima, and S. Fujimoto, *Pairing symmetries of multiple superconducting phases in UTe<sub>2</sub>: Competition between ferromagnetic and antiferromagnetic fluctuations*, Phys. Rev. B

- 109**, 064516 (2024).
- [89] S. K. Yip and J. A. Sauls, *Circular dichroism and birefringence in unconventional superconductors*, J. Low. Temp. Phys. **86**, 257 (1992).
- [90] H. Ueki, M. Ohuchi, and T. Kita, *Charging in a Superconducting Vortex Due to the Three Force Terms in Augmented Eilenberger Equations*, J. Phys. Soc. Jpn **87**, 044704 (2018).
- [91] Y. Masaki, *Vortex charges and impurity effects based on quasi-classical theory in an s-wave and a chiral p-wave superconductor*, Phys. Rev. B **99**, 054512 (2019).
- [92] D. Rainer and J. A. Sauls, *Strong-Coupling Theory of Superconductivity*, (World Scientific, Singapore, 1995) pp. 45-78, arXiv: 1809.05264 (2018).
- [93] A. V. Balatsky, I. Vekhter, and J.-X. Zhu, *Impurity-induced states in conventional and unconventional superconductors*, Rev. Mod. Phys. **78**, 373 (2006).
- [94] P. J. Hirschfeld, P. Wölfle, and D. Einzel, *Consequences of resonant impurity scattering in anisotropic superconductors: Thermal and spin relaxation properties*, Phys. Rev. B **37**, 83 (1988).
- [95] M. J. Graf, S.-K. Yip, J. A. Sauls, and D. Rainer, *Electronic thermal conductivity and the Wiedemann-Franz law for unconventional superconductors*, Phys. Rev. B **53**, 15147 (1996).
- [96] A. B. Vorontsov and I. Vekhter, *Unconventional superconductors under a rotating magnetic field. II. Thermal transport*, Phys. Rev. B **75**, 224502 (2007).
- [97] M. Eschrig, *Distribution functions in nonequilibrium theory of superconductivity and Andreev spectroscopy in unconventional superconductors*, Phys. Rev. B **61**, 9061 (2000).
- [98] G. D. Mahan, *Many-Particle Physics* (Springer Science & Business Media, 2013).